Spectral incremental dynamic methodology for nonlinear structural systems endowed with fractional derivative elements subjected to fully non-stationary stochastic excitation

Peihua Ni[1], Ioannis P. Mitseas[2,3,*], Vasileios C. Fragkoulis[4], Michael Beer[4,5,6]

[1]*Department of Civil and Environmental Engineering, National University of Singapore, 1 Engineering Drive 2, Singapore 117576, Singapore*

[2]*School of Civil Engineering, University of Leeds, Leeds LS2 9JT, UK*

[3]*School of Civil Engineering, National Technical University of Athens, Iroon Polytechneiou 9, Zografou, Athens 15780, Greece*

[4]*Department of Civil and Environmental Engineering, University of Liverpool, Liverpool L69 3GH, UK*

[5]*Institute for Risk and Reliability, Leibniz Universität Hannover, Callinstr. 34, Hannover 30167, Germany*

[6]*International Joint Research Center for Resilient Infrastructure & International Joint Research Center for Engineering Reliability and Stochastic Mechanics, Tongji University, Shanghai 200092, China*

Abstract

A novel spectral incremental dynamic analysis methodology for analysing structural response in nonlinear systems with fractional derivative elements is presented, aligning with modern seismic design codes, like Eurocode 8. Drawing inspiration from the concept of fully non-stationary stochastic processes, the vector of the imposed seismic excitations is characterised by time and frequency evolving power spectra stochastically compatible with elastic response spectra of specified damping ratio and ground acceleration. The proposed method efficiently determines the nonlinear system time-dependent probability density functions for the non-stationary system response amplitude by employing potent nonlinear stochastic dynamics concepts, such as stochastic averaging and statistical linearization. Unlike traditional incremental dynamic analysis curves found in the literature, the herein proposed method introduces a three-dimensional alternative counterpart, that of stochastic engineering demand parameter surfaces, providing with higher-order statistics of the system response. An additional noteworthy aspect involves the derivation of response evolutionary power spectra as function of spectral acceleration, offering a deeper insight into the underlying system dynamics. Besides its capabilities, the method maintains

*I.Mitseas@leeds.ac.uk

the coveted element of a particularly low associated computational cost, increasing its attractiveness and practicality among diverse applications of engineering interest. Numerical examples comprising the bilinear hysteretic model endowed with fractional derivative elements subject to an Eurocode 8 elastic design spectrum demonstrate the capabilities and reliability of the proposed methodology. Its accuracy is assessed by juxtaposing the derived results with germane Monte Carlo Simulation data.

Keywords: Nonlinear stochastic dynamics; Earthquake engineering; Incremental dynamic analysis; Fractional derivative; Statistical linearization; Stochastic averaging

1 Introduction

In the realm of structural engineering, encountering diverse nonlinearities is commonplace, accentuating the need of meticulously capturing the underlying nonlinear mechanisms dictating structural behaviour [1, 2]. Conventional structural dynamics predominantly relies on integer-order derivatives and integrals, yet constantly growing demands for more versatile and sophisticated modelling considering intricate temporal dependencies underscore a logical transition towards advanced mathematical tools such as fractional calculus [3, 4]. Although fractional calculus can be historically traced back to the exchanges between L'Hôpital and Leibniz, its practical integration into engineering modelling materialised in the early twentieth century. Among their numerous applications, fractional calculus' theoretical concepts have proven beneficial in the field of engineering, where several approaches with different advantages and limitations have been developed to assess the stochastic response of systems endowed with fractional derivative elements (e.g., [5, 6, 7, 8, 9]). More specifically, fractional models are predominantly used in civil engineering due to their ability to effectively capture the viscoelastic behaviour of materials over a wide frequency range while requiring only a limited number of model parameters. In this context, modal analysis resembling treatments (e.g., [10, 11]), as well as relevant numerical integration schemes (e.g., [12]), have been proposed for determining the response of linear structural multi-DOF systems with fractional order damping when subjected to arbitrary inputs, such as those resulting from earthquake-induced ground motions. Moreover, a multitude of research endeavours focusing on seismic isolation, vibration control, and energy harvesting applications demonstrate the capacity of fractional calculus to enhance system modelling in various instances of structural engineering interest

[13, 14, 15, 16, 17, 18, 19, 20, 21, 22, 23, 24, 25]. Indeed, achieving a more realistic representation of engineering dynamical systems often requires the incorporation of complex nonlinear relationships coupled with the utilisation of fractional calculus to model structural/material behaviour with higher levels of precision. Additionally, the mathematical treatment of excitations as non-stationary stochastic processes contributes to a more realistic depiction leading to the establishment of a robust foundation for formulating realistic structural analysis and design procedures (e.g., [26, 27, 28, 29, 30, 31]).

The emerging concept of Performance-Based Engineering (PBE) finds application in various fields, including civil engineering (for buildings and infrastructure), mechanical engineering, and other domains where the performance of systems under consideration is critical. This approach allows for more tailored and efficient designs that meet specific performance goals rather than adhering strictly to prescriptive codes and specifications. In addition, it considers the dynamic and evolving nature of engineering challenges incorporating a thorough consideration of the involved uncertainties (e.g., [32, 33, 34, 35]). In earthquake engineering, Incremental Dynamic Analysis (IDA) is a commonly used method for determining the functional relationship between the excitation-related variables, known as intensity measures (IMs), and the system response-related variables, known as engineering demand parameters (EDPs) in a PBE context [36]. The outcome of this coupling takes the form of an IDA curve which corresponds to a specific ground motion record, while each point on the curve is associated with a distinct scaled ground motion intensity level along with the corresponding magnitude of the structural system response. Note, in passing, that the determination of this functional relationship is typically associated with a specific computational cost which can render the process particularly cumbersome (e.g., [37, 38]). Conducting, however, IDA within a fully stochastic framework imposing demands for higher-order statistical quantities of the response such as the Probability Density Function (PDF), requires a resource-intensive Monte Carlo Simulation (MCS) framework that involves the generation of a high number of IDA curves. The latter is necessary for a robust statistical characterisation of the EDP. Notably, circumventing conventional brute force implementation of the IDA methodology under an MCS context, a number of research efforts has been recently raised utilising advanced concepts and tools of random vibration theory (e.g., [39, 35]).

There is evident value in exploring nuanced and more efficient methodologies to address the challenge of determining the functional relationship between IMs and EDPs of systems featuring nonlinearity and hysteretic behaviours, particularly when fractional derivative elements are incorporated within a PBE frame-

work. This paper proposes an approximate spectral incremental dynamic analysis technique for nonlinear structural systems endowed with fractional derivative elements subjected to fully non-stationary seismic excitations defined in accordance with contemporary aseismic codes provisions, such as Eurocode 8 (e.g., [40, 41]). The proposed approach is developed by resorting to potent nonlinear stochastic dynamics principles, specifically leveraging the stochastic averaging and the statistical linearization methodologies. Statistical linearization has been one of the most versatile methodologies for determining the stochastic response of engineering systems [42, 43, 44]. It has found a wide range of applications over the last decades (e.g., [45]), while the standard method has also been extended to account for systems with singular matrices and constraints (e.g., [46]). The extensive use of the method is due to the simplicity of its application, as well as to its capacity to treat a wide variety of systems exhibiting nonlinear and/or hysteretic behaviours. On the other hand, the stochastic averaging method has demonstrated its effectiveness in deriving vibration response approximate solutions for lightly damped systems under wide-band random excitations [47, 48, 49]. It has been successfully used, among others, to predict approximately the response of quasi-integrable Hamiltonian systems to bounded noise excitations [50]; to analyse strongly nonlinear systems endowed with fractional derivative terms, as well as systems subjected to combined deterministic and stochastic excitations [51, 52, 53]; to study the dynamics of ships in random seas [54]; to determine the response of nonlinear energy harvesting devices [55]; while a novel stochastic averaging-based technique has been proposed in [56] to evaluate the response displacement amplitude of single-DOF systems. The combination of statistical linearization and stochastic averaging methodologies facilitates the efficient determination of the probability density function for the non-stationary response of the nonlinear system. The developed methodology introduces a stochastic incremental dynamic analysis surface that yields reliable higher-order statistics of the system response. An additional notable feature is the derivation of the response evolutionary power spectrum as a function of spectral acceleration, providing with a more informative and comprehensive understanding of the underlying system dynamics at a minimum computational cost. Lastly, the developed method employs an incremental mechanisation, akin to the one used in the standard implementation of IDA. This ensures compatibility through the scaling of intensity while aligning with established practices, adding to its practicality of adoption in diverse engineering scenarios. The herein developed approach can be construed as an extension of the work in [39] to account for systems with fractional derivative terms subjected to aseismic code-compliant non-stationary stochastic excitations.

In the remainder of this paper, Sections 2.1 to 2.3 delve into the mathematical background that supports the developed framework. Following this, Section 2.4 provides insightful commentary on noteworthy features and the practical application of the proposed technique. Section 3 demonstrates the application of the framework through an illustrative example involving a structural system comprising the bilinear hysteretic model endowed with fractional derivative elements subject to a Eurocode 8 elastic design spectrum. The accuracy of the proposed technique is assessed by juxtaposing the derived results with pertinent MCS data obtained from nonlinear response time-history analysis (RHA). Finally, Section 4 succinctly outlines the main conclusions drawn from the present study.

2 Mathematical formulation

This segment details the mathematical intricacies involved in developing the proposed efficient spectral incremental dynamic methodology tailored for nonlinear structural systems endowed with fractional derivative elements. Special attention has been devoted to explaining the various simplifications and assumptions made to enhance numerical efficiency. To ensure that the presentation of the theoretical background material remains coherent without sacrificing readability, a brief introduction on fundamental concepts associated with generating stochastic processes compatible with Eurocode 8 elastic design spectrum is included in the following Subsection 2.1.

2.1 Derivation of evolutionary power spectrum compatible with an assigned elastic design spectrum

Several approaches have been developed in the literature for deriving stochastic process power spectra that are compatible in a stochastic sense with response spectra defined by aseismic codes; see [57, 58, 59, 60, 61] for some indicative references. In this section, the most important elements of a computationally efficient approach [41] for the derivation of design spectrum compatible evolutionary power spectra are included for completeness. Regardless of the specific method employed for this derivation, it is crucial to emphasise that the evolutionary power spectrum (EPS) and the associated non-stationary stochastic process serve solely as mathematical tools to represent the seismic input action. This representation is defined in terms of an elastic pseudo-acceleration response spectrum, and it plays

a key role in the subsequent review of the proposed coupled stochastic averaging and statistical linearization step.

Following the principles outlined in [41], the non-stationary excitation stochastic process $\ddot{x}_g(t)$ consists of two main components: a fully non-stationary segment $\ddot{x}_g^R(t)$ which is modelled using a real recorded earthquake time-history, and a time-modulated quasi-stationary corrective segment $\ddot{x}_g^S(t)$ representing a stationary zero mean Gaussian stochastic process; that is

$$\ddot{x}_g(t) = a\ddot{x}_g^R(t) + \varphi(t)\ddot{x}_g^S(t), \tag{1}$$

where a is the scaling coefficient, and $\varphi(t)$ is a time-modulating function such that [62]

$$\varphi(t) = \begin{cases} \left(\frac{t}{t_1}\right)^2, & t < t_1 \\ 1, & t_1 \leq t \leq t_2 \\ \exp\left[-\beta_m(t-t_2)\right], & t > t_2 \end{cases}, \tag{2}$$

with $t_2 = t_1 + T_s$, where t_1 and t_2 are the time instants when the Husid function [63] is equal to 0.05 and 0.95, respectively; β_m defines the decay of the modulating function. Lastly, T_s corresponds to the temporal segment of the strong part of the imposed seismic action where stationarity can be reasonably assumed. Subsequently, the following approximate relationship can be established for the linear response spectra in question,

$$S(\omega, \zeta; a_g^0) = \sqrt{a^2 S^R(\omega, \zeta; a_g^0)^2 + S^S(\omega, \zeta; a_g^0)^2}, \tag{3}$$

where $S^R(\omega, \zeta; a_g^0)$ and $S^S(\omega, \zeta; a_g^0)$ are the response spectra corresponding to a quiescent linear oscillator subjected to $\ddot{x}_g^R(t)$ and $\ddot{x}_g^S(t)$, respectively; a_g^0 stands for the imposed level of peak ground acceleration, whereas the scaling coefficient is

$$a = \min\left\{\frac{S(\omega, \zeta, a_g^0)}{S^R(\omega, \zeta; a_g^0)}\right\} \in (0, 1]. \tag{4}$$

The nonlinear equation that forms the foundation for relating a damped pseudo-acceleration response spectrum to a one-sided power spectrum associated with the stationary corrective segment of the Gaussian kind in the frequency domain (see Eq. (3)) reads

$$S^S(\omega_0, \zeta_0; a_g^0) = \eta_{x^S}\omega_0^2\sqrt{\lambda_{0,x^S}(\omega_0, \zeta_0; a_g^0)}. \tag{5}$$

In Eq. (5), η_{x^S} and λ_{0,x^S} are the peak factor and the variance of the response process $x^S(t)$ of a viscously damped quiescent linear oscillator with natural frequency

ω_0 and damping ratio ζ_0 subjected to $\ddot{x}_g^S(t)$. The nth order response spectral moment of the stationary corrective segment that appears in Eq. (5) reads

$$\lambda_{n,x^S}(\omega_0,\zeta_0;a_g^0)=\int_0^\infty \omega^n \frac{1}{(\omega_0^2-\omega^2)^2+(2\zeta_0\omega_0\omega)^2} G^S(\omega,\zeta_0;a_g^0)\mathrm{d}\omega. \tag{6}$$

The peak factor η_{x^S} is related with the concept of first-passage problem [64] and can be determined by the following semi-empirical expression

$$\eta_{x^S}(T_s,p)=\sqrt{2\ln\left\{2\mu_{x^S}\left[1-\exp\left(-\delta_{x^S}^{1.2}\sqrt{\pi\ln(2\mu_{x^S})}\right)\right]\right\}}, \tag{7}$$

where the mean zero crossing rate μ_{x^S} and the spread factor δ_{x^S} of the stationary corrective segment are defined as

$$\mu_{x^S}=\frac{T_s}{2\pi}\sqrt{\frac{\lambda_{2,x^S}}{\lambda_{0,x^S}}}(-\ln p)^{-1} \tag{8}$$

and

$$\delta_{x^S}=\sqrt{1-\frac{\lambda_{1,x^S}^2}{\lambda_{0,x^S}\lambda_{2,x^S}}}, \tag{9}$$

respectively. In Eq. (7), the probability p is specifically chosen to be 0.5. This choice ensures that the generated $S^S(\omega,\zeta_0;a_g^0)$ in Eq. (5) can be conceived as the median damped pseudo-acceleration response spectrum. The interested reader is directed to [41] for more details. Next, relying on the approximate expression [64]

$$\lambda_{0,x^S}(\omega_0,\zeta_0;a_g^0)=\frac{G^S(\omega_0,\zeta_0;a_g^0)}{\omega_0^3}\left(\frac{\pi}{4\zeta_0}-1\right)+\frac{1}{\omega_0^4}\int_0^{\omega_0} G^S(\omega,\zeta_0;a_g^0)\mathrm{d}\omega \tag{10}$$

and manipulating Eq. (5) gives

$$S^S(\omega_0,\zeta_0;a_g^0)=\eta_{x^S}^2\omega_0 G^S(\omega_0,\zeta_0;a_g^0)\left(\frac{\pi}{4\zeta_0}-1\right)+\eta_{x^S}^2\int_0^{\omega_0} G^S(\omega,\zeta_0;a_g^0)\mathrm{d}\omega. \tag{11}$$

Then, approximating numerically the integral based on a frequency domain discretisation of N frequency points $\omega_i=\omega_b^l+(i-0.5)\Delta\omega$, with $i=1,2,\ldots,N$ and $\omega_i\in(\omega_b^l,\omega_b^u)$, yields [65, 66]

$$G^S(\omega_i,\zeta_0;a_g^0)= \begin{cases} 0, & \omega_i\le\omega_b^l \\ \frac{4\zeta_0}{\omega_i\pi-4\zeta_0\omega_{i-1}}\left(\frac{(S^S(\omega_0,\zeta_0;a_g^0))^2}{\eta_{x^S}^2}-\Delta\omega\sum_{k=1}^{i-1}G^S(\omega_k,\zeta_0;a_g^0)\right), & \omega_b^l<\omega_i<\omega_b^u \end{cases} \tag{12}$$

Following the determination of the power spectrum $G^S(\omega, \zeta_0; a_g^0)$ in the range (ω_b^l, ω_b^u), the simulation of a non-stationary spectrum compatible acceleration time-history can be obtained resorting to the spectral representation method [67]. That is

$$\ddot{x}_g^{(j)}(t) = a\ddot{x}_g^R(t) + \varphi(t) \sum_{i=1}^{N_a} \sqrt{4G^S(i\Delta\omega, \zeta_0; a_g^0)\Delta\omega}\, \cos\left(i\Delta\omega t + \theta_i^{(j)}\right), \quad (13)$$

where $\theta_i^{(j)}$ are independent random phases uniformly distributed in the interval $[0, 2\pi)$, and N_a is the number of the considered harmonics. The corresponding EPS $G^{ES}(\omega, \zeta_0, t; a_g^0)$ of the non-stationary stochastic excitation process $\ddot{x}_g(t)$ is provided in terms of the non-separable EPS $G^R(\omega, \zeta_0, t; a_g^0)$ and the time-modulated separable power spectrum $G^S(\omega, \zeta_0; a_g^0)$ of the corrective term in the form

$$G^{ES}(\omega, \zeta_0, t; a_g^0) = a^2 G^R(\omega, \zeta_0, t; a_g^0) + \varphi(t)^2 G^S(\omega, \zeta_0; a_g^0). \quad (14)$$

The non-separable EPS $G^R(\omega, \zeta_0, t; a_g^0)$ can be obtained by various techniques [68, 69, 70, 71], such as Short-Time Fourier Transform and Wavelets Transform. To improve the matching between the response spectrum from the simulations and the target pseudo-acceleration response spectrum, the following iterative scheme for the corrective term is utilised

$$G^{S(j)}(\omega, \zeta_0; a_g^0) = G^{S(j-1)}(\omega, \zeta_0; a_g^0) \left[\frac{S(\omega, \zeta_0; a_g^0)^2}{\tilde{S}^{(j-1)}(\omega, \zeta_0; a_g^0)^2}\right], \quad (15)$$

where $\tilde{S}^{(j)}(\omega, \zeta_0; a_g^0)$ is the mean response spectrum of the non-stationary stochastic excitation process $\ddot{x}_g(t)$ at a specific level of peak ground acceleration a_g^0 in the jth iteration. For a more detailed presentation as well as a pertinent commentary on the topic, the interested reader may resort to [65, 41]. The nonlinear stochastic dynamics technique discussed in the following subsections operates independently from the herein presented approach which only works as a necessary first numerical step to represent the seismic input action with respect to contemporary aseismic codes provisions. This is accomplished through the generation of evolutionary power spectra characterising the underlying code-compliant stochastic excitation processes appropriately aligned with various levels of peak ground acceleration.

2.2 Determination of the equivalent linear system

The equation of motion of a stochastically excited quiscent single-degree-of-freedom (SDOF) system with fractional derivative elements is given by

$$\ddot{x}(t) + \beta \mathcal{D}_{0,t}^{\alpha} x(t) + g(t, x, \dot{x}) = \ddot{x}_g(t), \tag{16}$$

where $x(t)$ denotes the system response displacement and a dot over a variable corresponds to differentiation with respect to time. Further, $g(t, x, \dot{x})$ is a nonlinear function representing the hysteretic behaviour of the system and $\mathcal{D}_{0,t}^{\alpha} x(t)$ denotes the Caputo fractional derivative of order α defined as [72]

$$\mathcal{D}_{0,t}^{\alpha} x(t) = \frac{1}{\Gamma(1-\alpha)} \int_0^t \frac{\dot{x}(\tau)}{(t-\tau)^{\alpha}} \mathrm{d}\tau, \tag{17}$$

where $0 < \alpha < 1$, and $\Gamma(\cdot)$ is the Gamma function. β is a damping coefficient given by $\beta = 2\zeta_0 \omega_0^{2-\alpha}$, with ω_0 and ζ_0 denoting the natural frequency and damping ratio of the corresponding linear oscillator, respectively. Finally, $\ddot{x}_g(t)$ is a non-stationary stochastic seismic acceleration process, whose EPS $G^{ES}(\omega, \zeta_0, t; a_g^0)$ is compatible with a target pseudoacceleration response spectrum $S(\omega, \zeta_0; a_g^0)$.

Next, the nonlinear fractional SDOF system in Eq. (16) is linearised by resorting to a combination of the stochastic averaging and statistical linearization methodologies [73, 30]. In this context, assuming that the system is lightly damped, its response follows a pseudo-harmonic behaviour, such that [47]

$$x(t) = A(t) \cos(\omega(A) t + \psi(t)) \tag{18}$$

and

$$\dot{x}(t) = -\omega(A) A(t) \sin(\omega(A) t + \psi(t)). \tag{19}$$

In Eqs. (18) and (19), $A(t)$ and $\psi(t)$ denote the system response amplitude and phase, respectively, whereas $\omega(A)$ corresponds to the amplitude-dependent natural frequency. Given the pseudo-harmonic response assumption, $A(t)$ and $\psi(t)$ are considered as approximately constant over one cycle of oscillation, since they are slowly-varying quantities with respect to time [47]. Analytical expressions for the response amplitude and phase are derived by manipulating Eqs. (18) and (19). These are [74]

$$A^2(t) = x^2(t) + \left(\frac{\dot{x}(t)}{\omega(A)} \right)^2 \tag{20}$$

and

$$\psi(t) = -\omega(A)t - \arctan\left(\frac{\dot{x}(t)}{x(t)\omega(A)}\right), \tag{21}$$

respectively.

Next, an amplitude-dependent linearisation of the nonlinear fractional SDOF system in Eq. (16) is applied [42]. The latter is re-written for simplicity in the form

$$\ddot{x}(t) + \beta_0\dot{x}(t) + h_0(t, x, \mathcal{D}^{\alpha}_{0,t}x, \dot{x}) = \ddot{x}_g(t), \tag{22}$$

where

$$h_0(t, x, \mathcal{D}^{\alpha}_{0,t}x, \dot{x}) = \beta D^{\alpha}_{0,t}x(t) + g(t, x, \dot{x}) - \beta_0\dot{x}(t) \tag{23}$$

and $\beta_0 = 2\zeta_0\omega_0$ is a damping coefficient. In passing, it is noted that the intermediate step in Eq. (22) is adopted to facilitate the treatment of the fractional order term during the linearisation process [73, 30]. An equivalent linear system is then defined as

$$\ddot{x}(t) + (\beta_0 + \beta(A))\,\dot{x}(t) + \omega^2(A)x(t) = \ddot{x}_g(t), \tag{24}$$

where $\beta(A)$ and $\omega(A)$ denote the amplitude dependent equivalent linear damping and stiffness elements. Subsequently, forming the difference between Eqs. (22) and (24) and minimising it in the mean square sense yields [73, 75, 30]

$$\beta(A) = \frac{1}{A\omega(A)}S(A) + \frac{\beta}{\omega^{1-\alpha}(A)}\sin\left(\frac{\alpha\pi}{2}\right) - \beta_0 \tag{25}$$

and

$$\omega^2(A) = \frac{1}{A}F(A) + \beta\omega^{\alpha}(A)\cos\left(\frac{\alpha\pi}{2}\right), \tag{26}$$

where

$$S(A) = -\frac{1}{\pi}\int_0^{2\pi} z(A\cos\phi, -A\omega(A)\sin\phi)\sin\phi\mathrm{d}\phi, \tag{27}$$

and

$$F(A) = \frac{1}{\pi}\int_0^{2\pi} z(A\cos\phi, -A\omega(A)\sin\phi)\cos\phi\mathrm{d}\phi, \tag{28}$$

with $\phi(t) = \omega(A)t + \psi(t)$.

Considering then that $A(t)$ defines a non-stationary stochastic process, it can be deduced that the amplitude-dependent equivalent elements given by Eqs. (25) and (26) define also a set of non-stationary stochastic processes. Therefore, applying the expectation operator to Eqs. (25) and (26) leads to the corresponding time-varying mean values [74]. These are evaluated by

$$\beta_{eq}(t) = \int_0^{\infty} \beta(A)p(A, t)\mathrm{d}A \tag{29}$$

and

$$\omega_{eq}^2(t) = \int_0^\infty \omega^2(A) p(A,t) \mathrm{d}A, \tag{30}$$

respectively, where $p(A,t)$ denotes the non-stationary response amplitude PDF. Clearly, the evaluation of the time-varying equivalent elements in Eqs. (29) and (30) depends on the computation of $p(A,t)$. For this, motivated by the Rayleigh form of the linear SDOF system stationary response amplitude PDF [76], a corresponding expression was proposed in [74] for nonlinear systems subjected to evolutionary stochastic excitation. The latter has been further extended in [30] to account for nonlinear SDOF systems endowed with fractional derivative elements. It is given by

$$p(A,t) = \frac{\sin\left(\frac{\alpha\pi}{2}\right) A}{\omega_0^{1-\alpha} c(t)} \exp\left(\frac{\sin\left(\frac{\alpha\pi}{2}\right)}{\omega_0^{1-\alpha}} \frac{A^2}{2c(t)}\right), \tag{31}$$

where $c(t)$ denotes a time-dependent coefficient to be determined. The determination of $c(t)$ is attained by resorting to a stochastic averaging treatment of Eq. (24). Specifically, substituting Eq. (31) into the associated Fokker-Planck equation

$$\begin{aligned} \frac{\partial p(A,t)}{\partial t} = & -\frac{\partial}{\partial A}\left\{\left(-\frac{1}{2}(\beta_0 + \beta_{eq}(t))A + \frac{\pi G^{ES}(\omega_{eq}(t), t; a_g^0)}{2\omega_{eq}^2(t) A}\right) p(A,t)\right\} \\ & + \frac{1}{4}\frac{\partial}{\partial A}\left\{\frac{\pi G^{ES}(\omega_{eq}(t), t; a_g^0)}{\omega_{eq}^2(t)} \frac{\partial p(A,t)}{\partial A} + \frac{\partial}{\partial A}\left(\frac{\pi G^{ES}(\omega_{eq}(t), t; a_g^0)}{\omega_{eq}^2(t)} p(A,t)\right)\right\}, \end{aligned} \tag{32}$$

and manipulating leads to

$$\dot{c}(t) = -(\beta_0 + \beta_{eq}(c(t)))c(t) + \left(\frac{\sin\left(\frac{\alpha\pi}{2}\right)}{\omega_0^{1-\alpha}}\right) \frac{\pi G^{ES}(\omega_{eq}(c(t)), \zeta_0, t; a_g^0)}{\omega_{eq}^2(c(t))}. \tag{33}$$

Eq. (33) is a deterministic first-order nonlinear ordinary differential equation, which can be readily solved by the Runge–Kutta numerical integration scheme. Hence, computing $c(t)$ leads to the computation of the response amplitude PDF in Eq. (31), which in turn yields the equivalent linear elements in Eqs. (29) and (30).

Finally, the equivalent elements given by Eqs. (25) and (26) are approximately constant over one cycle of oscillation, due to their slowly-varying in time nature. Therefore, it can be proved that [77]

$$S_{xx}(\omega, t) = \int_0^\infty S_{xx}(\omega, t|A) p(A,t) \mathrm{d}A, \tag{34}$$

where

$$S_{xx}(\omega, t|A) = \frac{G^{ES}(\omega, \zeta_0, t; a_g^0)}{(\omega^2(A) - \omega^2)^2 + (\omega\beta(A))^2} \tag{35}$$

corresponds to the response EPS of a linear oscillator possessing natural frequency equal to $\omega(A)$ and damping element equal to $\beta(A)$. In this context, combining Eqs. (34) and (35) with Eqs. (25), (26) and (31), the joint time-frequency response EPS $S_{xx}(\omega, t)$ is expressed as a function of the EPS $G^{ES}(\omega, \zeta_0, t; a_g^0)$ of the non-stationary stochastic excitation process $\ddot{x}_g(t)$.

2.3 Proposed methodology for code-compliant stochastic incremental dynamic analysis

Many engineering systems of genuine interest can be effectively represented as SDOF systems, as noted in [42]. In this context, a quiescent nonlinear SDOF system endowed with fractional derivative elements is considered in the ensuing analysis. The system is base-excited by a response spectrum compatible acceleration stochastic process $\ddot{x}_g(t)$ whose dynamic behaviour is governed by Eq. (16). The non-stationary acceleration process $\ddot{x}_g(t)$ is characterised in the frequency domain by an associated EPS $G^{ES}(\omega, \zeta_0, t; a_g^0)$ compatibly defined with Eurocode 8 provisions. An incremental mechanisation analogous to the one used in standard IDA technique is employed herein, where a_g^0 operates as the scaled image of the excitation magnitude. In the present study, the selected EDP is that of the time-dependent response displacement amplitude $A(t)$ at the most critical time instant t_{in}. The t_{in} stands for the time instant when the parameter $c(t)$ found in Eq. (33) reaches its maximum value leading $p(A, t_{in}; a_g^0)$ in Eq. (31) to get its most broadband form. In this regard, the response amplitude PDF at t_{in} with respect to a specific level of the scaled excitation a_g^0 is given by

$$p(A, t_{in}; a_g^0) = \frac{\sin\left(\frac{\alpha\pi}{2}\right) A}{\omega_0^{1-\alpha} c(t_{in})} \exp\left(\frac{\sin\left(\frac{\alpha\pi}{2}\right)}{\omega_0^{1-\alpha}} \frac{A^2}{2c(t_{in})}\right). \tag{36}$$

Generating $p(A, t_{in}; a_g^0)$ for each scaled level of excitation a_g^0 enables the efficient determination of the stochastic IDA response amplitude PDF surface, encompassing valuable higher order statistics within a fully probabilistic perspective. By manipulating Eqs. (34) and (36), we obtain the response power spectrum with respect to a specified level of excitation a_g^0 at the most critical time instant t_{in}

$$G_{xx}(\omega, t_{in}, a_g^0) = \int_0^\infty \frac{G^{ES}(\omega, \zeta_0, t_{in}; a_g^0)}{(\omega^2(A) - \omega^2)^2 + (\omega\beta(A))^2} p(A, t_{in}; a_g^0) \mathrm{d}A. \tag{37}$$

Eq. (37) defines $G_{xx}(\omega, t_{in}; a_g^0)$ as the system response EPS for a time instant t_{in} under a specific ground acceleration level a_g^0 at a minimum computational cost. The aforementioned relation facilitates the determination of the effective response power spectrum, showcasing evolutionary traits as a function of spectral acceleration. Specifically, the mechanisation of the proposed spectral incremental dynamic analysis methodology to determine the stochastic response EDP-based IDA and the response EPS-based IDA surfaces comprises the following steps:

1. The excitation EPS $G^{ES}(\omega, \zeta_0, t; a_g^0)$ is derived in a stochastically compatible manner with a given elastic pseudo-acceleration response spectrum of specified damping ratio and scaled ground acceleration a_g^0.
2. Following the proposed stochastic averaging and linearisation method shown in Section 2.2, the maximum value $c_{max}(t_{in})$ and the corresponding time instant t_{in} are determined by Eqs. (29), (30) and (33).
3. The response EDP PDF and the response EPS at t_{in} for a specific level of excitation a_g^0 are determined by Eqs. (36) and (37), respectively.
4. Steps 1 to 3 are repeated for the scaled images of the excitation a_g^0 to determine the stochastic response EDP-based IDA and the response EPS-based IDA surfaces.

2.4 Discussion on attributes of the proposed methodology

This discussion delves into various notable aspects, including advantages, limitations and potential practical applications of the proposed spectral incremental dynamic analysis methodology. In comparison to existing state-of-the-art approaches in the literature, the proposed stochastic dynamics methodology exhibits several noteworthy features: (i) accommodating nonlinear structural systems with hysteretic behaviour; (ii) addressing complex and more sophisticated modelling requirements resorting to fractional calculus concepts; (iii) modelling ground motion as a vector of code-compliant fully non-stationary stochastic processes, avoiding challenges associated with selecting and scaling suites of earthquake records. Note, in passing, that this issue remains controversial in the relevant literature [78]; (iv) reducing bias by not relying on a limited number of subjectively selected seismic motion records; (v) determining higher-order statistics through the response EDP-based IDA surface, rather than solely estimating mean and standard deviation currently being the norm in the literature; (vi) being computationally efficient compared to nonlinear RHA for compatible ground motion records. Note that a reliable statistical description of an EDP is normally associated with a resource-intensive MCS framework involving the generation of

a high number of IDA curves; (vii) providing with a response EPS-based IDA surface which enables the monitoring of the dynamic character of the structural system. Specifically, the nonlinear characteristics are identified through a dual-faceted approach, encompassing both the stochastic response EPS-based surface and the time-variant equivalent linear elements. This foundation underpins a system identification framework, providing insights into both the frequency and time domain. An element which could be especially useful for a number of reasons such as tracking the system nonlinear character as well as tracing moving resonance phenomena (e.g., [79, 80, 30]). Note that this significant operation cannot be determined following typical nonlinear RHA. Relevant remarks should be provided regarding potential limitations in the method's expected level of accuracy for highly nonlinear and low-performance scenarios. The combination of stochastic averaging and statistical linearization methodologies may compromise accuracy in such cases. Notably, the method imposes no restrictions on the excitation process, except for the Gaussian assumption [42].

3 Illustrative application

The bilinear hysteretic force-deformation law is a common approach to emulate the behaviour of structural systems and members to seismic forces (e.g., [81, 16, 66, 42, 82, 1]). In this section, a bilinear hysteretic oscillator with fractional derivative elements subject to Eurocode 8 elastic pseudo-acceleration response spectra serves as the numerical example to demonstrate and validate the reliability of the proposed stochastic dynamics methodology. The obtained results are compared and found in good agreement with corresponding outcomes derived by nonlinear RHA in an MCS-based context. The imposed Eurocode 8 elastic design spectra are shown in the Appendix A.

3.1 Bilinear hysteretic SDOF system under code-compliant evolutionary stochastic seismic excitation

The equation of motion for a SDOF system featuring nonlinearity through a bilinear hysteretic model and incorporating fractional derivative elements is under consideration. The system's restoring force is expressed as

$$g(t, x(t), \dot{x}(t)) = \gamma k x(t) + (1-\gamma) k x_y z(t), \tag{38}$$

with

$$x_y \dot{z}(t) = \dot{x}\{1 - \Phi(\dot{x}(t))\Phi(z(t) - 1) - \Phi(-\dot{x}(t))\Phi(-z(t) - 1)\}, \tag{39}$$

where $\Phi(\cdot)$ denotes the Heaviside step function; γ is the post-yield to pre-yield stiffness ratio; z is an auxiliary state and x_y is the yielding displacement.

Considering Eqs. (25) and (26), the amplitude-time-dependent equivalent damping $\beta(A(t))$ and natural frequency $\omega(A(t))$ are given by

$$\beta(A(t)) = \frac{(1-\gamma)\omega_0^2 S_0(A)}{A\omega(A)} + \frac{\beta}{\omega^{1-\alpha}(A)} \sin\left(\frac{\alpha\pi}{2}\right) - \beta_0 \tag{40}$$

and

$$\omega^2(A(t)) = \omega_0^2 \left[\gamma + \frac{(1-\gamma)F_0(A)}{A} + \beta\omega^{\alpha}(A)\cos\left(\frac{\alpha\pi}{2}\right)\right], \tag{41}$$

where

$$S_0(A(t)) = \begin{cases} \frac{4x_y}{\pi}\left(1 - \frac{x_y}{A}\right), & A > x_y \\ 0, & A \leq x_y \end{cases} \tag{42}$$

$$F_0(A(t)) = \begin{cases} \frac{A}{\pi}\left[\Lambda - \frac{1}{2}\sin(2\Lambda)\right], & A > x_y \\ A, & A \leq x_y \end{cases}, \tag{43}$$

and $\cos(\Lambda) = 1 - \frac{2x_y}{A}$.

Next, considering the non-stationary response amplitude PDF in Eq. (31) and ensemble averaging Eqs. (40) and (41), the time-dependent equivalent linear properties for the bilinear SDOF system with fractional derivative elements are given by [30, 16]

$$\begin{aligned} \beta_{eq}(c(t)) = &-\beta_0 + \frac{\beta\sin^2(\frac{\alpha\pi}{2})}{\omega_0^{1-\alpha}c(t)} \int_0^{\infty} \frac{A}{\omega^{1-\alpha}(A)} \exp\left(-\frac{\sin(\frac{\alpha\pi}{2})}{\omega_0^{1-\alpha}} \frac{A^2}{2c(t)}\right) \mathrm{d}A \\ &+ \frac{4x_y\omega_0^2(1-\gamma)\sin(\frac{\alpha\pi}{2})}{\pi\omega_0^{1-\alpha}c(t)} \int_{x_y}^{\infty} \frac{1 - \frac{x_y}{A}}{\omega(A)} \exp\left(-\frac{\sin(\frac{\alpha\pi}{2})}{\omega_0^{1-\alpha}} \frac{A^2}{2c(t)}\right) \mathrm{d}A \end{aligned} \tag{44}$$

and

$$\begin{aligned} \omega_{eq}^2(c(t)) = &\omega_0^2 - (1-\gamma)\omega_0^2 \left\{\exp\left(-\frac{{x_y}^2\sin(\frac{\alpha\pi}{2})}{2c(t)\omega_0^{1-\alpha}}\right) - \frac{\sin(\frac{\alpha\pi}{2})}{\pi\omega_0^{1-\alpha}c(t)} \right. \\ &\left. \times \int_{x_y}^{\infty} (\Lambda - \frac{1}{2}\sin(2\Lambda))A \exp\left(-\frac{\sin(\frac{\alpha\pi}{2})}{\omega_0^{1-\alpha}} \frac{A^2}{2c(t)}\right) \mathrm{d}A\right\} \\ &+ \frac{\beta\sin(\frac{\alpha\pi}{2})\cos(\frac{\alpha\pi}{2})}{\omega_0^{1-\alpha}c(t)} \int_0^{\infty} \omega^{\alpha}(A)A \exp\left(-\frac{\sin(\frac{\alpha\pi}{2})}{\omega_0^{1-\alpha}} \frac{A^2}{2c(t)}\right) \mathrm{d}A, \end{aligned} \tag{45}$$

respectively.

3.2 Determination of the stochastic response-based IDA surfaces

The Eurocode 8 elastic pseudo-acceleration design spectrum $S(\omega, \zeta; a_g^0)$ for soil type B serves as the baseline input spectrum. Additionally, the non-stationary attributes of the excitation are modelled using the recorded time history from the El Centro site during the SOOE (NS) component of the Imperial Valley earthquake on May 18, 1940. Scaled excitations are determined as $a_g^0 = g \times [0.10, 0.20, 0.40, 0.60, 0.80, 1.00, 1.20]$, where g represents the acceleration of gravity. Further, Fig. 1 shows the generated EPS $G^{ES}(\omega, \zeta_0, t; a_g^0)$ compatible with a Eurocode 8 type B design spectrum $S(\omega, \zeta_0; a_g^0)$ for $a_g^0 = 0.20g$ and for $a_g^0 = 0.40g$. The following parameter values have been used for the bilinear oscillator: $\omega_0 = 10\, rad/s$, $\zeta_0 = 0.05$, $\alpha = 0.5$, $\gamma = 0.2$ and $x_y = 0.03\ m$. The methodology outlined in Sections 2.1 to 2.3 enables the efficient determination of the stochastic response EDP-based IDA and the response EPS-based IDA surfaces at a considerably low computational cost. Notably, the time instances t_{in} vary based on the scaled image of the ground acceleration a_g^0, following the criterion of the maximum value $c_{max}(t_{in})$ in step 2.

Next, Fig. 2 shows the generated time-dependent response amplitude PDF $p(A, t)$ based on Eqs. (31) and (33) for a seismic excitation level $a_g^0 = 0.40g$. To assess the achieved level of accuracy, comparisons with pertinent MCS data are included and shown in Fig. 3. Specifically, utilising the spectral representation method [83], an ensemble of $10,000$ acceleration time histories is generated, compatible with the reference response spectrum corresponding to the specific scaled image of the excitation a_g^0. Subsequently, the governing equation of motion Eq. (16) subject to the above ensemble of accelerograms is numerically solved by resorting to an L1-algorithm [15]. Next, the response amplitude PDF $p(A, t_{in}; a_g^0)$ at critical time instants t_{in} when the response variance indicated parameter reaches its maximum value $c_{max}(t_{in})$ is selected as the EDP. In Figs. 4(a) and 4(b), the response amplitude PDFs $p(A, t; a_g^0)$ at two separate time instants, namely t_p and t_{in} for scaled images of peak ground acceleration are compared with relevant outcomes derived from MCS. The t_p denotes the time instant when the excitation gets its highest value. In this regard, $t_p = 1.80s$ while t_{in} for different scale images of accelerations $0.10g, 0.40g, 0.60g$ are equal to $2.66s, 2.28s$ and $2.34s$, respectively. As expected, $t_{in} > t_p$ indicating the reasonable existence of an output/input lag

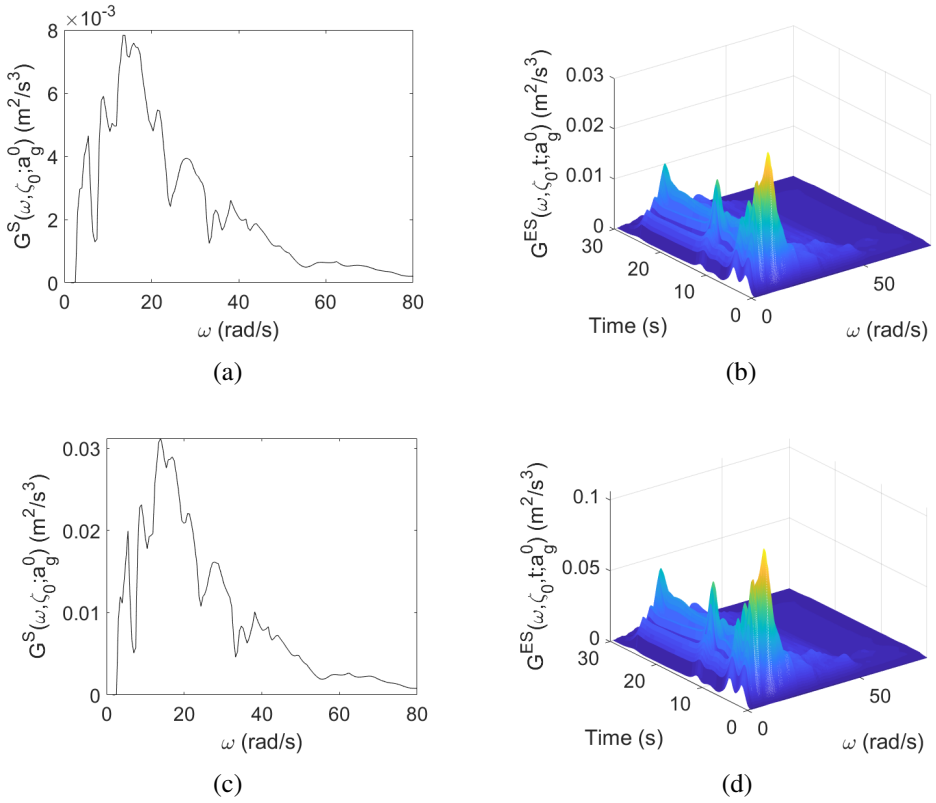

Fig. 1. (a) Generated power spectrum $G^S(\omega, \zeta_0 = 0.05; a_g^0 = 0.20g)$ corresponding to the stationary process $\ddot{x}_g^S(t)$; (b) Excitation EPS $G^{ES}(\omega, \zeta_0, t; a_g^0 = 0.20g)$ compatible with an Eurocode 8 type B design spectrum $S(\omega, \zeta_0 = 0.05; a_g^0 = 0.20g)$; (c) Generated power spectrum $G^S(\omega, \zeta_0 = 0.05; a_g^0 = 0.40g)$ corresponding to the stationary process $\ddot{x}_g^S(t)$; (d) Excitation EPS $G^{ES}(\omega, \zeta_0, t; a_g^0 = 0.40g)$ compatible with an Eurocode 8 type B design spectrum $S(\omega, \zeta_0 = 0.05; a_g^0 = 0.40g)$.

dependent on the magnitude of the excitation as well as the performed degree of system nonlinearity. In passing, it is noted that the corresponding time instants t_{in} differ with respect to the scaled image of the ground acceleration a_g^0.

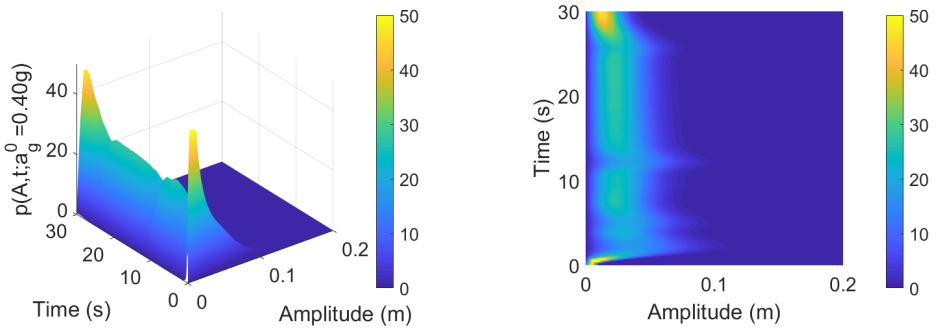

Fig. 2. Response amplitude PDF $p(A, t; a_g^0 = 0.40g)$ by the proposed analytical method compatible with an Eurocode 8 type B design spectrum $S(\omega, \zeta = 0.05; a_g^0)$: (a) 3D view; (b) planar view.

Further, following the proposed spectral incremental dynamic methodology, the stochastic response EDP-based IDA surface is shown in Figs. 5(a) and 5(b). The accuracy of the proposed technique is assessed by juxtaposing the derived results with germane MCS data shown in Figs. 6(a) and 6(b). Considering the approximations involved in the proposed approach, it can be clearly stated that the obtained results are in good agreement with the MCS-based estimates. The response EPS-based IDA surface is shown in Figs. 7(a) and 7(b). It is noted that exceeding an intensity threshold signals a gradual transition from elastic into the plastic region. The noted break, which is expressed with a transition to lower values of frequency, is indicative of the system stiffness degradation. It is noteworthy that the proposed stochastic dynamics method provides with an insight into the underlying dynamic character of the system; this significant operation cannot be determined following typical nonlinear RHA.

Furthermore, a fractional bilinear oscillator with a different nonlinear factor parameter value compared to the previous example is considered. The corresponding parameter values for the target system are the same as in the previous case, except for $\gamma = 0.5$. Similarly, using the proposed spectral incremental dynamical methodology, the response amplitude PDFs $p(A, t_p; a_g^0)$ and $p(A, t_{in}; a_g^0)$ at two distinct time instants t_p and t_{in}, for scaled images of peak ground acceler-

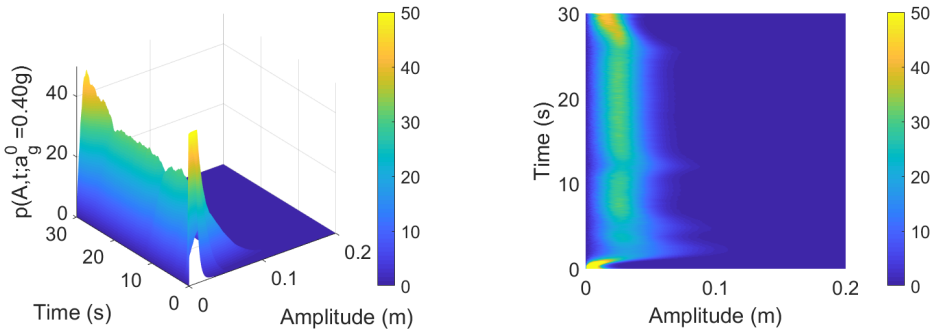

(a) (b)

Fig. 3. Response amplitude PDF $p(A, t; a_g^0 = 0.40g)$ by the MCS method $(10,000$ realisations) compatible with an Eurocode 8 type B design spectrum $S(\omega, \zeta = 0.05; a_g^0)$: (a) 3D view; (b) planar view.

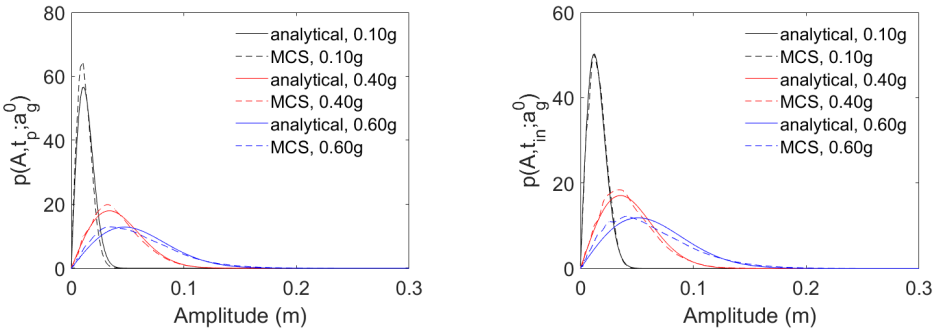

(a) (b)

Fig. 4. Response amplitude PDF $p(A, t; a_g^0)$ at separate time instants compatible with Eurocode 8 type B design spectrum $S(\omega, \zeta = 0.05; a_g^0)$ for different scaled images of ground accelerations $a_g^0 = 0.10g, 0.40g, 0.60g$; comparison between proposed methodology and MCS-based estimates $(10,000$ realisations): (a) $p(A, t; a_g^0)$ at t_p; (b) $p(A, t; a_g^0)$ at t_{in}.

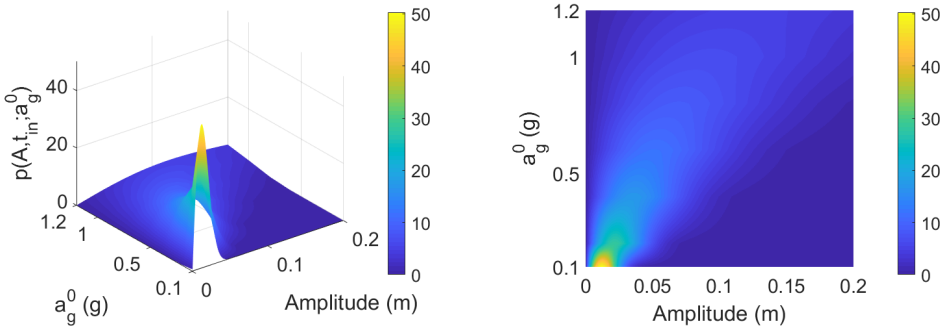

(a) (b)

Fig. 5. Stochastic response EDP-based IDA surface of a bilinear hysteretic SDOF system with fractional derivative elements by the proposed analytical method: (a) 3D view; (b) planar view.

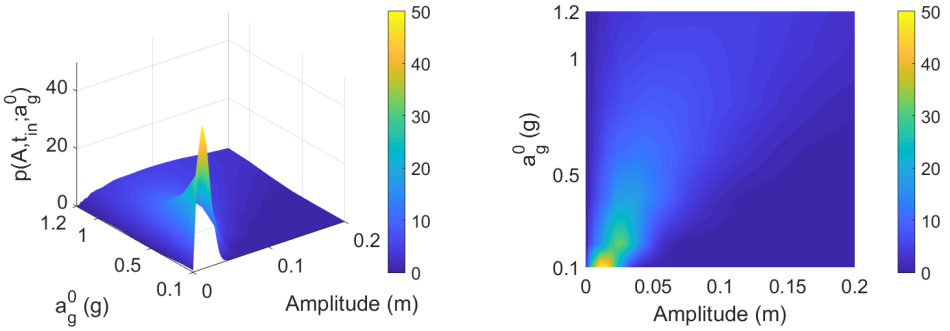

(a) (b)

Fig. 6. Stochastic response EDP-based IDA surface of a bilinear hysteretic SDOF system with fractional derivative elements by the MCS method ($10,000$ realisations): (a) 3D view; (b) planar view.

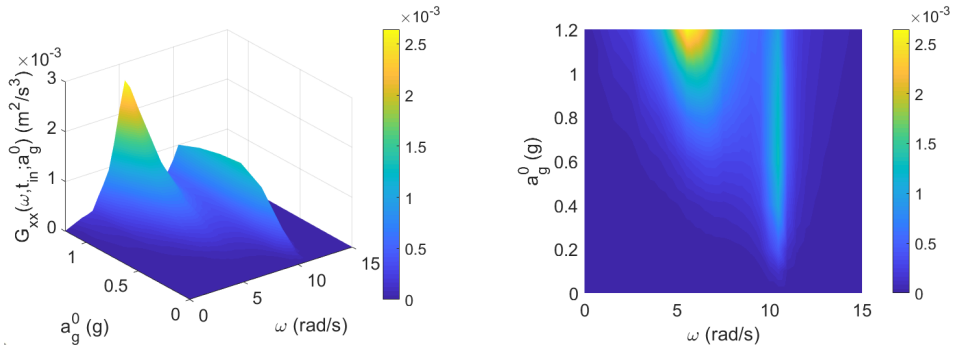

(a) (b)

Fig. 7. Response EPS stochastic IDA surface of a bilinear hysteretic SDOF system with fractional elements: (a) 3D view; (b) planar view

ation are shown in Figs. 8(a) and 8(b), respectively. A comparison with MCS data ($10,000$ realisations) is performed to demonstrate the noted good levels of accuracy. In this case, t_{in} for different acceleration scales $0.10g, 0.40g, 0.60g$ are $2.72s, 2.32s, 2.34s$, which occur later than t_p. This input/output lag indicates the presence of nonlinearity. Next, the stochastic response EDP-based IDA surfaces of the target system using the proposed methodology and the MCS method are shown in Figs. 9 and 10, respectively. The results obtained by the proposed analytical method are in good agreement with the MCS data. Additionally, the response EPS-based IDA surface of the target system is shown in Fig. 11. The transition of results considering the frequency content of the EPS, indicates that the system's behaviour gradually shifts from the elastic to the plastic range with increasing excitation acceleration, signifying relevant stiffness degradation. In this case study the noted stiffness degradation is kept in lower levels as compared to the case of ($\omega_0 = 10\ rad/s$, $\zeta_0 = 0.05$, $\alpha = 0.5$, $\gamma = 0.2$) due to the updated value of γ which corresponds to a system with a weaker nonlinear character.

Lastly, to illustrate the effects of nonlinearity, Figs. 12(a) and 12(b) present the time-variant equivalent linear natural frequencies $\omega_{eq}(t)$ and damping ratios $\zeta_{eq}(t)$ at t_{in} for the case studies of the target system discussed above for nonlinear factors $\gamma = 0.2$ and 0.5, respectively; see Eqs. (44) and (45) where $\zeta_{eq}(t_{in}) = \frac{\beta_0 + \beta_{eq}(t_{in})}{2w_{eq}(t_{in})}$. Specifically, stronger nonlinear response due to marching towards higher excitation IM leads to heavier damped equivalent oscillators shifted towards lower frequencies for both cases. In agreement with the above argument, the range of equivalent linear elements in Fig. 12(a) which is associated with a system

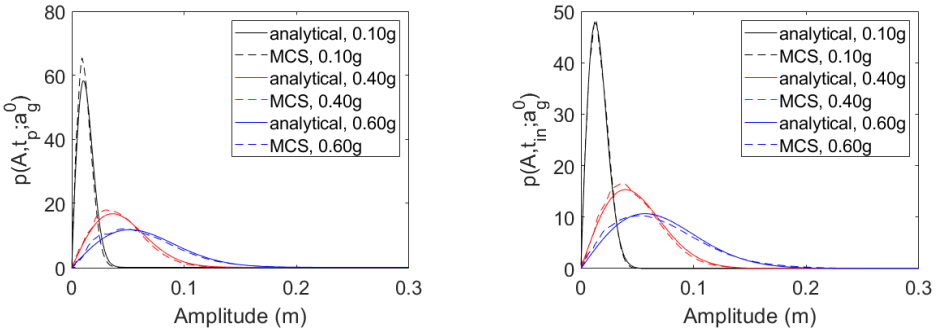

(a) (b)

Fig. 8. Response amplitude PDF $p(A, t; a_g^0)$ at separate time instants compatible with Eurocode 8 type B design spectrum $S(\omega, \zeta = 0.05; a_g^0)$ for different scaled images of ground accelerations $a_g^0 = 0.10g, 0.40g, 0.60g$; comparison between proposed methodology and MCS-based estimates $(10,000$ realisations): (a) $p(A, t; a_g^0)$ at t_p; (b) $p(A, t; a_g^0)$ at t_{in}.

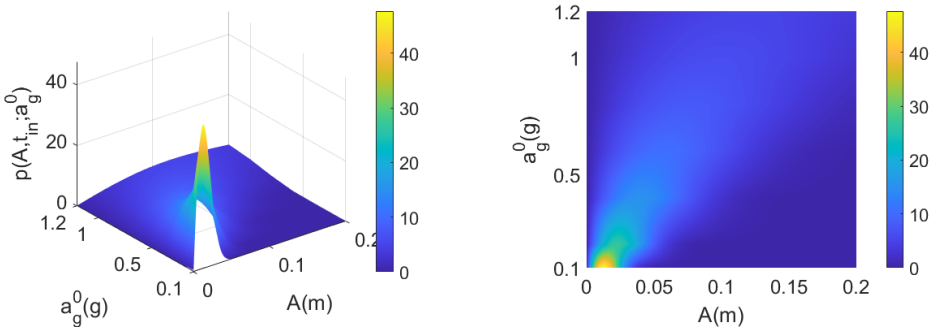

(a) (b)

Fig. 9. Stochastic response EDP-based IDA surface of a bilinear hysteretic SDOF system with fractional derivative elements by the proposed analytical method: (a) 3D view; (b) planar view.

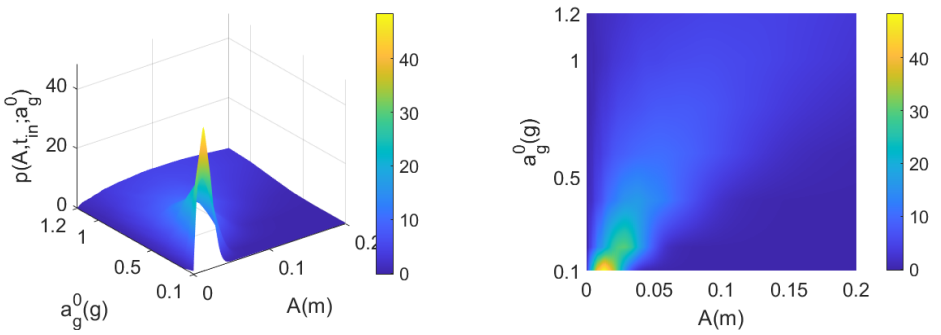

(a) (b)

Fig. 10. Stochastic response EDP-based IDA surface of a bilinear hysteretic SDOF system with fractional derivative elements by the MCS method $(10,000$ realisations): (a) 3D view; (b) planar view.

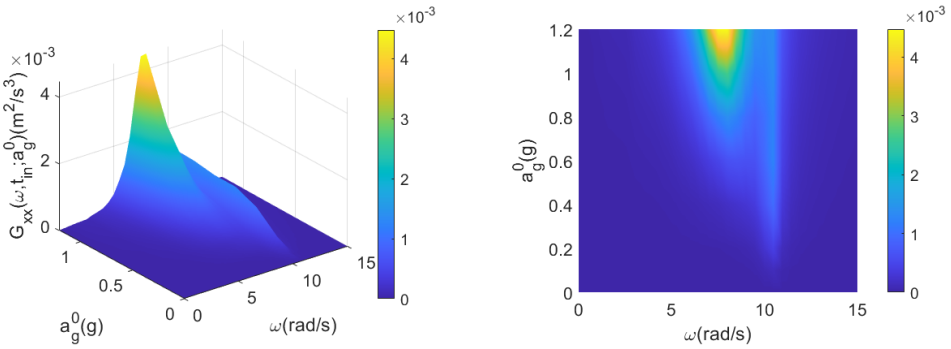

(a) (b)

Fig. 11. Response EPS stochastic IDA surface of a bilinear hysteretic SDOF system with fractional elements: (a) 3D view; (b) planar view

corresponding to higher degree of nonlinearity is higher than the one noted in Fig. 12(b).

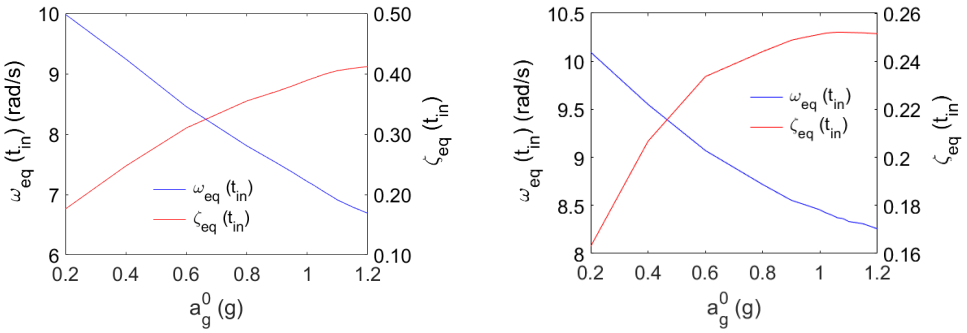

Fig. 12. Time-variant equivalent linear natural frequency and damping ratio at t_{in} for the target system ($\omega_0 = 10\,rad/s$, $\zeta_0 = 0.05$, $\alpha = 0.5$) with different nonlinear factors corresponding to different scales of the imposed excitation: (a) $\gamma = 0.2$; (b) $\gamma = 0.5$.

This fact indicates that the magnitude of nonlinearity affects the equivalent linear elements, as determined using the stochastic averaging and statistical linearization method. As expected, higher nonlinearity in the system leads to softer behaviour and results in a larger range for the corresponding equivalent linear elements.

3.3 Discussion on the impact of the fractional order in the system behaviour

In this section, the impact of the fractional order in the behaviour of the system under consideration is discussed. As test bed, the initial bilinear system with parameter values $\omega_0 = 10\,rad/s$, $\zeta_0 = 0.05$ and $\gamma = 0.2$ is studied. In this context, as shown in Figs. 13(a) to 13(d), by increasing the value of the fractional order from $\alpha = 0.2$ to $\alpha = 0.8$, meaning adding more damping to the system, results in a decreasing trend for the magnitudes of the corresponding generated response EPS. This kind of behaviour is clearly depicted considering the pertinent response EPS peaks. In addition, conclusions around the impact of the fractional order in the stiffness/stiffness degradation of the system can be drawn from Figs. 13(a) to

13(d). As it is reasonably expected, increasing the fractional order of the system from $\alpha = 0.2$ to $\alpha = 0.8$, leads to less stiff systems, thus, the corresponding frequencies where the generated EPS present their peaks show a small tendency marching towards lower values.

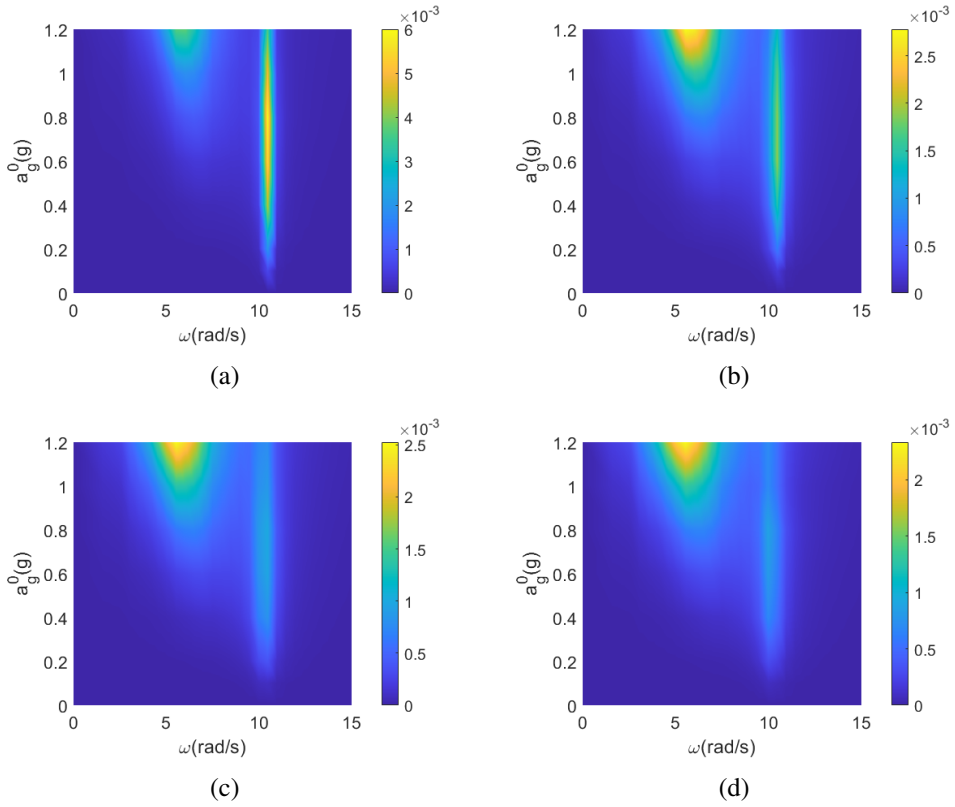

Fig. 13. Response EPS stochastic IDA surface of a bilinear hysteretic SDOF system ($\omega_0 = 10 rad/s$, $\zeta_0 = 0.05$, $\gamma = 0.2$) for various values of the fractional order: (a) $\alpha = 0.2$; (b) $\alpha = 0.4$; (c) $\alpha = 0.6$; (d) $\alpha = 0.8$.

The nonlinear character of the system is monitored through a twofold mechanism which involves the stochastic response EPS-based surface as well as the time-variant equivalent linear elements which lay the foundation for a system identification character of the proposed methodology offering pertinent information in the frequency as well as in the time domain.

4 Concluding remarks

In this paper, a novel spectral IDA methodology has been developed for nonlinear structural systems featuring fractional derivative elements and subjected to a seismic excitation vector consistently aligned with contemporary aseismic codes provisions. In this regard, an incremental mechanisation akin to the one used in normal IDA ensures the necessary compatibility for pertinent structural engineering applications. Specifically, resorting to the concept of non-stationary stochastic processes, the imposed seismic excitation vector is provided in the form of evolutionary power spectra stochastically compatible with elastic pseudo-acceleration response spectra of specified damping ratio and scaled ground acceleration. Harnessing the potential of an efficient combination of the stochastic averaging and the statistical linearization methodologies, the response amplitude PDFs are determined in a competent and effective manner. Contrary to the current norm in the literature, the proposed stochastic dynamics methodology provides with the response EDP-based IDA surface. This leads to the computation of reliable higher-order statistics of the selected EDP, rather than simple estimates only of the mean and standard deviation. Notably, a particularly interesting attribute of the proposed methodology pertains to the derivation of the associated response EPS as a function of spectral acceleration. This is an important aspect as it performs structural behaviour monitoring considering excitation intensity, whereas it provides with an insight into the underlying dynamic character of the system. The nonlinear characteristics are identified through a dual-faceted approach, encompassing both the stochastic response EPS-based surface and the time-variant equivalent linear elements. This foundation underpins a system identification framework, providing relevant insights into both the frequency and time domain. Notably, monitoring the dynamic character of a structural system is unattainable following typical nonlinear RHA. Lastly, the associated low computational cost enhances its utility in various related performance-based engineering applications.

Regarding the limitations of the proposed framework, since the statistical linearization method is one of its critical components, considering the Gaussian assumption of the system response is inevitable [42]. Considering also that the system response follows a pseudo-harmonic behaviour prevents the application of the proposed framework to systems exhibiting strongly non-Gaussian response behaviours or systems with multiple static equilibrium positions [30]. Further, extending the proposed framework for the study of multi-DOF systems is also rather indirect, thus, it is identified as a potential field for future research. While alternative linearization techniques could be explored for addressing multi-DOF

systems, such approaches would primarily yield lower-order response statistics. In contrast, a key advantage of the proposed stochastic dynamics scheme lies in its ability to derive higher-order response statistics, which are crucial for accurately capturing the non-stationary character of the nonlinear response and generating the EDP-based IDA as well as the EPS stochastic IDA surfaces.

A numerical example featuring a bilinear model with fractional derivative elements demonstrates the methodology's reliability, while comparisons with MSC data validate the accuracy of the proposed code-compliant spectral IDA stochastic dynamics technique.

Declaration of competing interest

The authors declare that they have no known competing financial interests or personal relationships that could have appeared to influence the work reported in this paper.

Acknowledgment

The authors gratefully acknowledge the support by the Hellenic Foundation for Research and Innovation (Grant No. 1261), by the German Research Foundation (Grant No. FR 4442/2-1), by the National Natural Science Foundation of China (Grant No. 72271025), and by the Guangdong Basic and Applied Basic Research Foundation (Grant No. 2023A1515011532).

A Eurocode 8 design spectrum

The Eurocode 8 defines the elastic pseudo-acceleration response spectrum for linear oscillators with damping ratio ζ and natural period $T = 2\pi/\omega$ through the following expressions [40]

$$S(T,\zeta) = a_g^0 \times \begin{cases} S\left[1 + \frac{T}{T_B}(2.5\eta - 1)\right], & 0 \le T \le T_B \\ 2.5S\eta, & T_B \le T \le T_C \\ 2.5S\eta\frac{T_C}{T}, & T_C \le T \le T_D \\ 2.5S\eta\frac{T_C T_D}{T^2}, & T_D \le T \le T_E \\ S\frac{T_C T_D}{T^2}\left[2.5\eta + \frac{T-T_E}{T_F-T_E}(1-2.5\eta)\right], & T_E \le T \le T_F \\ S\frac{T_C T_D}{T^2}, & T_F \le T \end{cases}, \quad (46)$$

where

$$\eta = \sqrt{\frac{10}{5+\zeta}} \geq 0.55, \tag{47}$$

with a_g^0 denoting the peak ground acceleration, S denoting a soil-dependent amplification factor, and T_B, T_C, T_D, T_E and T_F corresponding to soil-dependent corner periods. For soil type B: $S = 1.20, T_B = 0.15, T_C = 0.5, T_D = 2.0, T_E = 5.0, T_F = 10$.

References

[1] A. Giaralis, P. D. Spanos, Effective linear damping and stiffness coefficients of nonlinear systems for design spectrum based analysis, Soil Dynamics and Earthquake Engineering 30 (9) (2010) 798–810.

[2] I. P. Mitseas, I. A. Kougioumtzoglou, A. Giaralis, M. Beer, A novel stochastic linearization framework for seismic demand estimation of hysteretic MDOF systems subject to linear response spectra, Structural Safety 72 (2018) 84–98.

[3] J. A. T. M. J. Sabatier, O. P. Agrawal, J. A. T. Machado, Advances in fractional calculus, Vol. 4, Springer, 2007.

[4] J. T. Machado, V. Kiryakova, F. Mainardi, Recent history of fractional calculus, Communications in nonlinear science and numerical simulation 16 (3) (2011) 1140–1153.

[5] A. Pirrotta, I. A. Kougioumtzoglou, A. Di Matteo, V. C. Fragkoulis, A. A. Pantelous, C. Adam, Deterministic and random vibration of linear systems with singular parameter matrices and fractional derivative terms, Journal of Engineering Mechanics 147 (6) (2021) 04021031.

[6] Y. Zhang, I. A. Kougioumtzoglou, F. Kong, A Wiener path integral technique for determining the stochastic response of nonlinear oscillators with fractional derivative elements: A constrained variational formulation with free boundaries, Probabilistic Engineering Mechanics 71 (2023) 103410.

[7] A. Di Matteo, P. D. Spanos, Determination of nonstationary stochastic response of linear oscillators with fractional derivative elements of rational order, Journal of Applied Mechanics (2023) 1–25.

[8] I. G. Mavromatis, I. A. Kougioumtzoglou, A reduced-order Wiener path integral formalism for determining the stochastic response of nonlinear systems with fractional derivative elements, ASCE-ASME Journal of Risk and Uncertainty in Engineering Systems, Part B: Mechanical Engineering 9 (3) (2023) 031201.

[9] D. Jerez, V. Fragkoulis, P. Ni, I. Mitseas, M. A. Valdebenito, M. G. Faes, M. Beer, Operator norm-based determination of failure probability of nonlinear oscillators with fractional derivative elements subject to imprecise stationary gaussian loads, Mechanical Systems and Signal Processing 208 (2024) 111043.

[10] T.-S. Chang, M. P. Singh, Seismic analysis of structures with a fractional derivative model of viscoelastic dampers, Earthquake Engineering and Engineering Vibration 1 (2002) 251–260.

[11] R. Lewandowski, Z. Pawlak, Response spectrum method for building structures with viscoelastic dampers described by fractional derivatives, Engineering Structures 171 (2018) 1017–1026.

[12] M. Singh, T.-S. Chang, H. Nandan, Algorithms for seismic analysis of MDOF systems with fractional derivatives, Engineering Structures 33 (8) (2011) 2371–2381.

[13] N. Makris, M. C. Constantinou, Fractional-derivative Maxwell model for viscous dampers, Journal of Structural Engineering 117 (9) (1991) 2708–2724.

[14] F. Rüdinger, Tuned mass damper with fractional derivative damping, Engineering Structures 28 (13) (2006) 1774–1779.

[15] C. G. Koh, J. M. Kelly, Application of fractional derivatives to seismic analysis of base-isolated models, Earthquake engineering & structural dynamics 19 (2) (1990) 229–241.

[16] I. A. Kougioumtzoglou, P. Ni, I. P. Mitseas, V. C. Fragkoulis, M. Beer, An approximate stochastic dynamics approach for design spectrum based response analysis of nonlinear structural systems with fractional derivative elements, International Journal of Non-Linear Mechanics 146 (2022) 104178.

[17] M. Di Paola, G. Failla, A. Pirrotta, A. Sofi, M. Zingales, The mechanically based non-local elasticity: an overview of main results and future challenges, Philosophical Transactions of the Royal Society A: Mathematical, Physical and Engineering Sciences 371 (1993) (2013) 20120433.

[18] Y. A. Rossikhin, M. V. Shitikova, Application of fractional calculus for dynamic problems of solid mechanics: novel trends and recent results, Applied Mechanics Reviews 63 (1) (2010).

[19] A. Di Matteo, F. L. Iacono, G. Navarra, A. Pirrotta, Innovative modeling of tuned liquid column damper motion, Communications in Nonlinear Science and Numerical Simulation 23 (1-3) (2015) 229–244.

[20] K. R. dos Santos, O. Brudastova, I. A. Kougioumtzoglou, Spectral identification of nonlinear multi-degree-of-freedom structural systems with fractional derivative terms based on incomplete non-stationary data, Structural Safety 86 (2020) 101975.

[21] H. H. Lee, C.-S. Tsai, Analytical model of viscoelastic dampers for seismic mitigation of structures, Computers & structures 50 (1) (1994) 111–121.

[22] J. Xu, J. Li, Stochastic dynamic response and reliability assessment of controlled structures with fractional derivative model of viscoelastic dampers, Mechanical Systems and Signal Processing 72 (2016) 865–896.

[23] F. Kong, Y. Zhang, Y. Zhang, Non-stationary response power spectrum determination of linear/non-linear systems endowed with fractional derivative elements via harmonic wavelet, Mechanical Systems and Signal Processing 162 (2022) 108024.

[24] A. Aprile, J. A. Inaudi, J. M. Kelly, Evolutionary model of viscoelastic dampers for structural applications, Journal of Engineering Mechanics 123 (1997) 551–560.

[25] A. A. Markou, G. D. Manolis, A fractional derivative zener model for the numerical simulation of base isolated structures, Bullettin of Earthquake Engineering 14 (2016) 283–295.

[26] I. P. Mitseas, M. Beer, Fragility analysis of nonproportionally damped inelastic MDOF structural systems exposed to stochastic seismic excitation, Computers & Structures 226 (2020) 106129.

[27] P. Ni, V. Fragkoulis, F. Kong, I. Mitseas, M. Beer, Non-stationary response of nonlinear systems with singular parameter matrices subject to combined deterministic and stochastic excitation, Mechanical Systems and Signal Processing 188 (2023) 110009.

[28] M. Barbato, J. Conte, Spectral characteristics of non-stationary random processes: Theory and applications to linear structural models, Probabilistic Engineering Mechanics 23 (4) (2008) 416–426.

[29] G. Deodatis, Non-stationary stochastic vector processes: seismic ground motion applications, Probabilistic engineering mechanics 11 (3) (1996) 149–167.

[30] V. C. Fragkoulis, I. A. Kougioumtzoglou, A. A. Pantelous, M. Beer, Non-stationary response statistics of nonlinear oscillators with fractional derivative elements under evolutionary stochastic excitation, Nonlinear Dynamics 97 (4) (2019) 2291–2303.

[31] V. C. Fragkoulis, I. A. Kougioumtzoglou, Survival probability determination of nonlinear oscillators with fractional derivative elements under evolutionary stochastic excitation, Probabilistic Engineering Mechanics 71 (2023) 103411.

[32] E. Tubaldi, M. Barbato, A. Dall'Asta, Performance-based seismic risk assessment for buildings equipped with linear and nonlinear viscous dampers, Engineering Structures 78 (2014) 90–99.

[33] I. P. Mitseas, I. A. Kougioumtzoglou, M. Beer, An approximate stochastic dynamics approach for nonlinear structural system performance-based multi-objective optimum design, Structural Safety 60 (2016) 67–76.

[34] A. D. Kiureghian, Non-ergodicity and PEER's framework formula, Earthquake engineering & structural dynamics 34 (13) (2005) 1643–1652.

[35] I. P. Mitseas, M. Beer, First-excursion stochastic incremental dynamics methodology for hysteretic structural systems subject to seismic excitation, Computers & Structures 242 (2021) 106359.

[36] D. Vamvatsikos, C. A. Cornell, Incremental dynamic analysis, Earthquake engineering & structural dynamics 31 (3) (2002) 491–514.

[37] D. Vamvatsikos, Performing incremental dynamic analysis in parallel, Computers & structures 89 (1-2) (2011) 170–180.

[38] D. Vamvatsikos, Seismic performance uncertainty estimation via IDA with progressive accelerogram-wise latin hypercube sampling, Journal of Structural Engineering 140 (8) (2014) A4014015.

[39] K. R. dos Santos, I. A. Kougioumtzoglou, A. T. Beck, Incremental dynamic analysis: a nonlinear stochastic dynamics perspective, Journal of Engineering Mechanics 142 (10) (2016) 06016007.

[40] CEN, Eurocode 8: Design of Structures for Earthquake Resistance - Part 1: General Rules, Seismic Actions and Rules for Buildings, Comité Européen de Normalisation, Brussels EN 1998-1: 2003 E. (2004).

[41] P. Cacciola, A stochastic approach for generating spectrum compatible fully nonstationary earthquakes, Computers & Structures 88 (15-16) (2010) 889–901.

[42] J. B. Roberts, P. D. Spanos, Random vibration and statistical linearization, Courier Corporation, 2003.

[43] S. H. Crandall, A half-century of stochastic equivalent linearization, Structural Control and Health Monitoring: The Official Journal of the International Association for Structural Control and Monitoring and of the European Association for the Control of Structures 13 (1) (2006) 27–40.

[44] L. Socha, Linearization methods for stochastic dynamic systems, Vol. 730, Springer Science & Business Media, 2007.

[45] C. Proppe, H. Pradlwarter, G. Schuëller, Equivalent linearization and Monte Carlo simulation in stochastic dynamics, Probabilistic Engineering Mechanics 18 (1) (2003) 1–15.

[46] I. A. Kougioumtzoglou, V. C. Fragkoulis, A. A. Pantelous, A. Pirrotta, Random vibration of linear and nonlinear structural systems with singular matrices: A frequency domain approach, Journal of Sound and Vibration 404 (2017) 84–101.

[47] J. B. Roberts, P. D. Spanos, Stochastic averaging: an approximate method of solving random vibration problems, International Journal of Non-Linear Mechanics 21 (2) (1986) 111–134.

[48] W. Q. Zhu, Stochastic averaging methods in random vibration, Applied Mechanics Reviews 41 (5) (1988) 189–199.

[49] W. Zhu, Recent developments and applications of the stochastic averaging method in random vibration (1996).

[50] Z. Huang, W. Zhu, Stochastic averaging of quasi-integrable Hamiltonian systems under bounded noise excitations, Probabilistic Engineering Mechanics 19 (3) (2004) 219–228.

[51] Z. Huang, W. Zhu, Y. Suzuki, Stochastic averaging of strongly non-linear oscillators under combined harmonic and white-noise excitations, Journal of Sound and Vibration 238 (2) (2000) 233–256.

[52] Z. Huang, X. Jin, Response and stability of a SDOF strongly nonlinear stochastic system with light damping modeled by a fractional derivative, Journal of Sound and Vibration 319 (3-5) (2009) 1121–1135.

[53] L. Chen, W. Zhu, Stochastic averaging of strongly nonlinear oscillators with small fractional derivative damping under combined harmonic and white noise excitations, Nonlinear Dynamics 56 (2009) 231–241.

[54] L. Dostal, E. Kreuzer, N. Sri Namachchivaya, Non-standard stochastic averaging of large-amplitude ship rolling in random seas, Proceedings of the Royal Society A: Mathematical, Physical and Engineering Sciences 468 (2148) (2012) 4146–4173.

[55] W.-A. Jiang, L.-Q. Chen, Stochastic averaging of energy harvesting systems, International Journal of Non-Linear Mechanics 85 (2016) 174–187.

[56] P. D. Spanos, I. A. Kougioumtzoglou, K. R. dos Santos, A. T. Beck, Stochastic averaging of nonlinear oscillators: Hilbert transform perspective, Journal of Engineering Mechanics 144 (2) (2018) 04017173.

[57] A. Giaralis, P. Spanos, Wavelet-based response spectrum compatible synthesis of accelerograms-Eurocode application (EC8), Soil Dynamics and Earthquake Engineering 29 (1) (2009) 219–235.

[58] P. T. Brewick, M. Hernandez-Garcia, S. F. Masri, A. W. Smyth, A data-based probabilistic approach for the generation of spectra-compatible time-history records, Journal of Earthquake Engineering 22 (8) (2018) 1365–1391.

[59] I. D. Gupta, M. D. Trifunac, Defining equivalent stationary PSDF to account for nonstationarity of earthquake ground motion, Soil Dynamics and Earthquake Engineering 17 (2) (1998) 89–99.

[60] P. D. Spanos, L. M. V. Loli, A statistical approach to generation of design spectrum compatible earthquake time histories, International Journal of Soil Dynamics and Earthquake Engineering 4 (1) (1985) 2–8.

[61] P. D. Spanos, A. Di Matteo, Z. H., Y. Q., X. z., Estimation of evolutionary power spectra of univariate stochastic processes by energy-based reckoning, Reliability Engineering & System Safety 245 (2024) 109962.

[62] P. C. Jennings, Equivalent viscous damping for yielding structures, Journal of the Engineering Mechanics Division 94 (1) (1968) 103–116.

[63] R. Husid, Características de terremotos. análisis general, Revista IDIEM 8 (1) (1969) ág–21.

[64] E. H. Vanmarcke, Structural response to earthquakes, in: Developments in Geotechnical Engineering, Vol. 15, Elsevier, 1976, pp. 287–337.

[65] P. Cacciola, P. Colajanni, G. Muscolino, Combination of modal responses consistent with seismic input representation, Journal of Structural Engineering 130 (1) (2004) 47–55.

[66] I. P. Mitseas, M. Beer, Modal decomposition method for response spectrum based analysis of nonlinear and non-classically damped systems, Mechanical Systems and Signal Processing 131 (2019) 469–485.

[67] M. Shinozuka, G. Deodatis, Simulation of stochastic processes by spectral representation (1991).

[68] L. Cohen, Time-frequency distributions-a review, Proceedings of the IEEE 77 (7) (1989) 941–981.

[69] J. P. Conte, B.-F. Peng, An explicit closed-form solution for linear systems subjected to nonstationary random excitation, Probabilistic Engineering Mechanics 11 (1) (1996) 37–50.

[70] P. D. Spanos, G. Failla, Evolutionary spectra estimation using wavelets, Journal of Engineering Mechanics 130 (8) (2004) 952–960.

[71] I. A. Kougioumtzoglou, I. Petromichelakis, A. F. Psaros, Sparse representations and compressive sampling approaches in engineering mechanics: A review of theoretical concepts and diverse applications, Probabilistic Engineering Mechanics 61 (2020) 103082.

[72] I. Podlubny, Fractional differential equations: an introduction to fractional derivatives, fractional differential equations, to methods of their solution and some of their applications, Elsevier, 1998.

[73] P. D. Spanos, A. Di Matteo, Y. Cheng, A. Pirrotta, J. Li, Galerkin scheme-based determination of survival probability of oscillators with fractional derivative elements, Journal of Applied Mechanics 83 (12) (2016).

[74] I. A. Kougioumtzoglou, P. D. Spanos, An approximate approach for nonlinear system response determination under evolutionary stochastic excitation, Current science (2009) 1203–1211.

[75] A. Di Matteo, P. D. Spanos, A. Pirrotta, Approximate survival probability determination of hysteretic systems with fractional derivative elements, Probabilistic Engineering Mechanics 54 (2018) 138–146.

[76] P.-T. D. Spanos, L. D. Lutes, Probability of response to evolutionary process, Journal of the Engineering Mechanics Division 106 (2) (1980) 213–224.

[77] I. A. Kougioumtzoglou, Stochastic joint time–frequency response analysis of nonlinear structural systems, Journal of Sound and Vibration 332 (26) (2013) 7153–7173.

[78] M. Grigoriu, Do seismic intensity measures (IMs) measure up?, Probabilistic Engineering Mechanics 46 (2016) 80–93.

[79] I. P. Mitseas, I. A. Kougioumtzoglou, P. D. Spanos, M. Beer, Nonlinear MDOF system survival probability determination subject to evolutionary stochastic excitation, Strojniski Vestnik-Journal of Mechanical Engineering 62 (7-8) (2016) 440–451.

[80] J. L. Beck, C. Papadimitriou, Moving resonance in nonlinear response to fully nonstationary stochastic ground motion, Probabilistic Engineering Mechanics 8 (3-4) (1993) 157–167.

[81] A. K. Chopra, C. Chintanapakdee, Inelastic deformation ratios for design and evaluation of structures: single-degree-of-freedom bilinear systems, Journal of structural engineering 130 (9) (2004) 1309–1319.

[82] K. Yang, P. Tan, H. Chen, J. Li, W. Zheng, A framework for nonlinear peak response evaluation from linear response spectra of base-isolated structures using the bilinear hysteretic model, Soil Dynamics and Earthquake Engineering 177 (2024) 108360.

[83] J. Liang, S. R. Chaudhuri, M. Shinozuka, Simulation of nonstationary stochastic processes by spectral representation, Journal of Engineering Mechanics 133 (6) (2007) 616–627.